2022 44th Annual International Conference of
the IEEE Engineering in Medicine & Biology Society (EMBC)
Scottish Event Campus, Glasgow, UK, July 11-15, 2022

2022 44th Annual International Conference of the IEEE Engineering in Medicine & Biology Society (EMBC) | 978-1-7281-2782-8/22/$31.00 ©2022 IEEE | DOI: 10.1109/EMBC48229.2022.9871270

Arterial Pulse Localization with Varying Electrode Sizes and Spacings in Wrist-Worn Bioimpedance Sensing

Jesse F. Phipps, Kaan Sel, *Student Member, IEEE*, Roozbeh Jafari, *Senior Member, IEEE*

***Abstract*— Bioimpedance has emerged as a promising modality to continuously monitor hemodynamic and respiratory physiological parameters through a non-invasive skin-contact approach. Bioimpedance sensors placed at the radial zone of the volar wrist provide sensitive operation to the blood flow of the underlying radial artery. The translation of bioimpedance systems into medical-grade settings for continuous hemodynamic monitoring, however, presents challenges when constraining the necessary sensing components to a minimal form factor while maintaining sufficient accuracy and precision of measurements. Thus, it is important to understand the effects of electrode configuration on bioimpedance signals when reducing them to a wearable form factor. Previous work regarding electrode configurations in bioimpedance does not address wearable constraints, nor do they focus on electrodes viable for wearable applications. In this study, we present empirical evidence of the effects of dry silver electrode sizes and spacings on the specificity and sensitivity of a wrist-worn bioimpedance sensor array. We found that wrist-worn bioimpedance systems for hemodynamic monitoring would benefit from reduced injection electrode spacings (up to a 392% increase in signal amplitude with a 50% decrease in spacing), increased sensing electrode spacings, and decreased electrode surface areas.**

***Clinical Relevance*— The work directly contributes towards the development of cuffless continuous blood pressure monitors with applications in clinical and ambulatory settings.**

I. Introduction

Continuous health monitoring is an essential part of prognostic and diagnostic medical practices both in healthy and disordered communities. Current medical grade systems provide sensitive and reliable but invasive and inconvenient measurement of complex cardiovascular (e.g., blood pressure, cardiac output, arterial compliance) and respiratory (e.g., respiration rate, breathing patterns) health parameters, making them impractical for long-term use. Wearable devices have become increasingly popular in recent years [1] as they offer noninvasive and convenient sensing of physiological parameters at the limbs (*e.g.*, wrist-worn). These devices can noninvasively measure blood flow at the arteries with the trade-off of limited sensitivity and specificity. Therefore, if the reliability and accuracy of wearables are improved, their measurements can reveal important information regarding cardiovascular health and has the potential to improve current diagnostic and prognostic medical practices.

Bioimpedance (Bio-Z) is a promising modality for monitoring physiological parameters. It offers a cuffless, noninvasive approach that is cost-effective, convenient, and supports wearable applications. Optical modalities (*e.g.*, photoplethysmography) are only sensitive to surface-level capillaries and capture hemodynamic changes that are neutralized [2], whereas a bioimpedance signal penetrates deep into the underlying tissues to capture arterial blood flow. Hence, bioimpedance sensor arrays placed above an artery can measure various complex hemodynamic and respiratory parameters including blood pressure [3], respiration rate [4], and arterial compliance [5]. However, bioimpedance measurements are scalar, and therefore it is challenging to localize the arterial pulsatile activity and optimize sensor placement for high-fidelity and robust operation. Therefore, it is of great importance to understand and predict the effects of spatial parameters within an electrode array configuration for wrist-worn bioimpedance applications. While previous studies have focused on the effects of electrode placement [6], [7], size, and spacing [8] on bioimpedance sensing depths, they do not address form factor constraints in the range of wrist-worn devices, for which they are substantial. Furthermore, previous work has focused on applications involving wet electrodes, which are not a viable solution for wearable devices due to electrode gel dehydration over time and skin irritation [9].

This study provides a thorough experimental assessment of the impact of electrode size and spacing in bioimpedance sensing on blood pressure pulse localization. Our contributions in this paper can be summarized as follows:

- Introducing an extensive experimental analysis of bioimpedance measurements with three different viable dry electrode sizes and seven different spacings for wrist-worn hemodynamic monitoring.
- Providing an assessment of the impact of electrode spacing and size on the sensitivity of bioimpedance sensing through experimental analysis of the bioimpedance signal at different spatial electrode placements and electrode sizes integrated into wristbands.
- Providing an assessment of the impact of electrode spacing and size to specificity of bioimpedance sensing through pulse transit time (PTT) measurements at each electrode configuration.

J.F. Phipps is with the Department of Computer Science and Engineering at Texas A&M University, College Station, Texas 77843, USA. (e-mail: jessefphipps@tamu.edu).

K. Sel is with the Department of Electrical and Computer Engineering at Texas A&M University, College Station, Texas, 77843, USA. (e-mail: ksel@tamu.edu)

R. Jafari is with the Departments of Biomedical Engineering, Computer Science and Engineering, and Electrical Engineering at Texas A&M University, College Station, Texas, 77843, USA. (e-mail: rjafari@tamu.edu).

II. Materials and Methods

A. Electrode design and fabrication

Bioimpedance technique requires a current injection to the skin through a pair of electrodes, and another pair of electrodes for picking up the voltage difference due the flow of electrical current through the tissue [10]. We fabricated a total of 10 unique four-electrode dry silver plates set in silicon with elastic bands attached to each side as shown in Fig. 1. Electrodes were cut from 0.33 mm thick silver strips and shaped into squares with the appropriate surface area. Wires were then soldered onto the silver electrodes to be connected to the Bio-Z XL board described in part C of this section. To capture a wide range of electrode placement configurations, we focused on Wenner and Wenner-Schlumberger spacing definitions, where Wenner configurations maintain equidistant on-center spacing, and Wenner-Schlumberger configurations possess unequal spacings between electrodes determined by a spacing coefficient n and a base spacing a as shown in Fig. 2.

For electrode contact areas, we used three Wenner configurations with equal on-center spacings of 10 mm and electrode contact areas of 9 mm^2, 25 mm^2, and 64 mm^2 with 1:1 aspect ratios. To analyze the impact of electrode spacings, the 7 remaining bands consisted of 25 mm^2 electrodes with spacings varying from 6 mm to 15 mm using Wenner configuration and with base spacings varying from 6 mm to 15 mm with Wenner-Schlumberger configurations, where the spacing coefficients vary from 0.5 to 1.5. To avoid an overlap

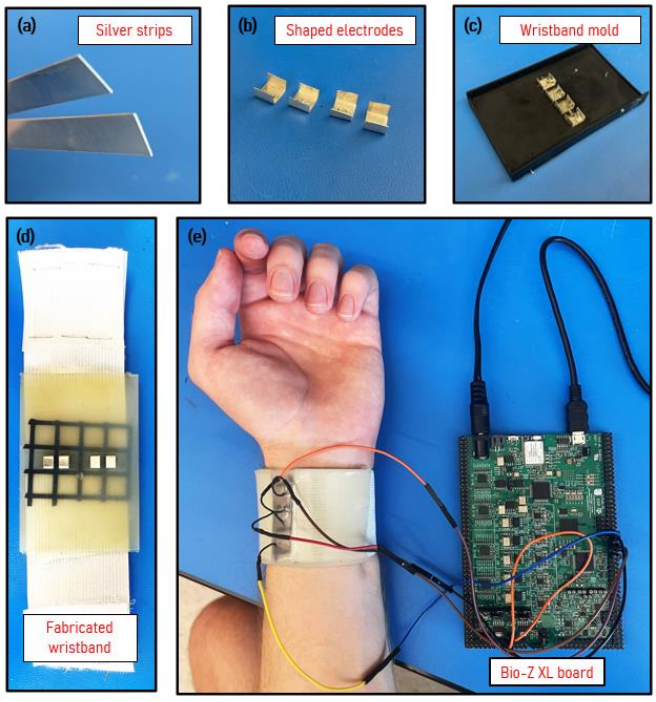

Figure 1. Fabrication process of the dry silver electrode wristbands used in this study. (a) Pure silver strips before cutting and shaping. (b) Cut and shaped electrodes (c) Cut and shaped silver electrodes in a wristband mold (d) A fully fabricated electrode wristband ready for use (e) Experimental setup showing the fabricated electrodes and the bioimpedance measurement system (i.e., Bio-Z XL board).

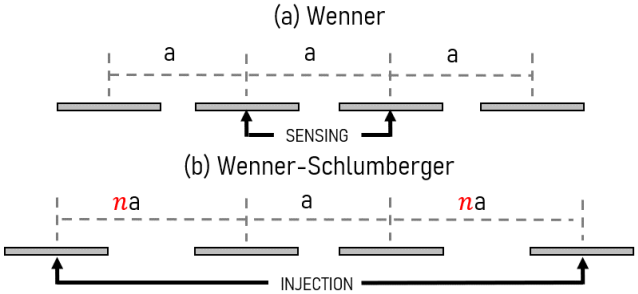

Figure 2. Electrode configuration selection strategies. (a) Wenner configuration corresponding to equal spacing between the electrodes. (b) Wenner-Schlumberger configuration with a spacing coefficient, n, between the injection and sensing electrodes. In a single-channel setup, two sensing electrodes are placed between two injection electrodes to capture changes in underlying tissue impedance. In a two-channel setup, four sensing electrodes are utilized, two for each channel, and are both placed between the injection electrodes.

of electrodes, the Wenner-Schlumberger configurations of spacing 6 mm did not include a spacing coefficient of 0.5. We shared the detailed list of all fabricated electrode configurations in Table 1.

For all bioimpedance measurements, we located the radial artery using an ultrasound Doppler device and aligned each electrode along the artery to capture the pulsatile activity due to the movement of the blood pressure pulse in the radial artery.

B. Electrode-skin impedance measurements

The electrode-skin impedance, also referred to as contact impedance, is an important factor that contributes to bioimpedance signal quality [11]. A contact impedance that is too high often leads to saturation of the injected sinusoid, which significantly degrades data quality. Thus, it is necessary to understand the effect of electrode contact areas on the impedance measured at the electrode-skin interface. For all contact impedance measurements, we used a Hioki LCR meter (IM3536, Hioki, Japan) and swept frequencies between 10 Hz and 1 MHz at five points per decade.

C. Bioimpedance signal acquisition

To capture the small variations in the bioimpedance signal that are due to the blood pressure pulse quasi-periodically travelling within the radial artery, we used a custom multi-

TABLE I
Electrode Band Parameters

Type	Surface Area (mm^2)	a (mm)	n
Wenner	9	10	1.0
	25	10	1.0
	64	10	1.0
	25	6	1.0
	25	15	1.0
Wenner-Schlumbeger	25	6	1.5
	25	10	0.6
	25	10	1.5
	25	15	0.5
	25	15	1.5

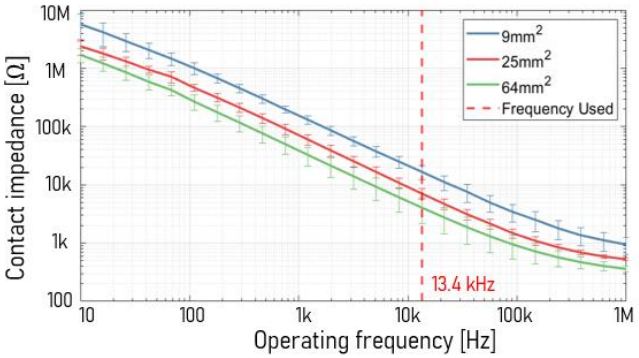

Figure 3. Electrode-skin impedance vs. the operating frequency for different electrodes sizes measured in surface areas. The injection frequency used in this study is shown by the dashed red line at 13.4 kHz, demonstrating the lowered skin impedance when using this frequency for each electrode surface area.

channel bioimpedance acquisition system, dubbed the Bio-Z XL board, as shown in Fig. 1 [4]. The Bio-Z XL board depends on an ARM Cortex M4 microcontroller that operates a high-frequency, 16-bit digital-to-analog converter (DAC8811, Texas Instruments, USA) with programmable gain and frequency to generate a 13.4 kHz sinusoidal voltage signal. This frequency of 13.4 kHz was selected due to low electrode-skin contact impedance (see Fig. 3) allowing a higher current injection (0.2 mA) within analog front end voltage supply limits (±5 V), in compliance with safety standards [12]. A higher frequency would allow a lower skin contact impedance, with the drawback of increased digital sampling rate and processing burden.

This signal is then converted to electric current with a precision amplifier (OPA211, Texas Instruments, USA) to be injected into the skin across the injection electrode pair. The board uses high-precision instrumentation amplifiers (AD8221, Analog Devices, USA) to amplify the signal captured at the voltage pick-up electrodes, followed by an anti-aliasing filter prior to sampling with a 24-bit analog-to-digital converter (ADS1278, Texas Instruments, USA) at 100 kSPS sampling rate. The digital signal is sent to a PC through USB communication for digital signal processing.

The digital recordings are I-Q demodulated in MATLAB to obtain the raw bioimpedance signal. To extract the changes in the bioimpedance signal due to blood, denoted as ΔBio-Z, we applied a 6th order Butterworth band-pass filter with low and high frequency cut-offs at 0.05 Hz and 6 Hz, respectively. The filter removes the DC component of the bioimpedance and baseband wandering from the signal, in addition to the removal of the high-frequency image noise that is generated in the process of I-Q demodulation. The resultant ΔBio-Z signal is a quasi-periodic waveform that decreases with the arrival of the blood under the sensing location, where the amplitude of this signal quantifies the sensitivity of the bioimpedance sensing to the blood pressure pulse. The data were then normalized for each subject from 0 – 1 to convey trends rather than report raw values, which differ between subjects due to anatomy.

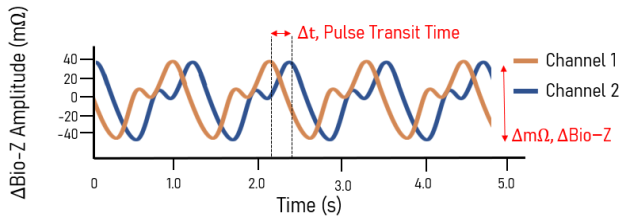

Figure 4. Visualizations of Pulse Transit Time (PTT) and ΔBio-Z on two Bio-Z waveforms. As seen, ΔBio-Z is the peak-to-peak mΩ of a Bio-Z signal, requiring only one channel. PTT, on the other hand, is the time difference between two waveforms captured at a fixed distance apart and requires two channels to be measured.

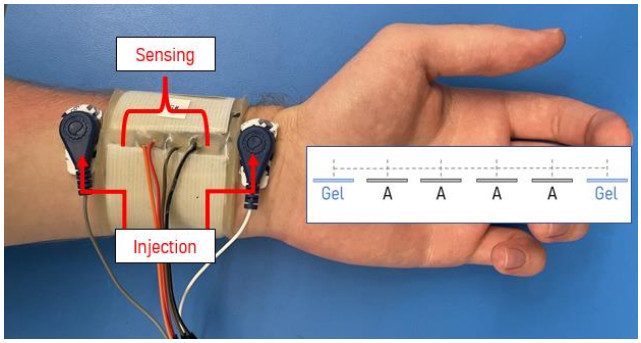

Figure 5. Electrode configuration for PTT measurements. "A" denotes the area of the silver sensing electrodes, whereas the gel electrodes remained constant. Note the use of constant spacing, where the only variable in the setup is the surface area of the square electrodes. This still causes electrode edges to become closer, while on-center spacing remains consistent.

D. Pulse transit time measurements

Pulse transit time (PTT) is a measure of the time it takes for a blood pressure pulse to travel from a distal to proximal location as seen in Fig. 4. PTT measurements can be used to extract blood pressure [13], an important biomarker of cardiovascular health. Placing two pairs of vicinal bioimpedance sensors can give a PTT measurement in a wearable form-factor, with a trade-off of very low PTT amplitude due to minimal separation between two sensing points. Conversely, with proper electrode placement, if pulse localization is achieved, this improved specificity to the pulse will increase the measured PTT. To measure PTT as a function of sensing electrode configurations, we placed two outer gel-based wet electrodes with the same separation across all measurements and used two fabricated bands having the same total sensor width with different electrode configurations to capture two ΔBio-Z signals (four silver electrodes, one ΔBio-Z signal from each consecutive pair) using the Bio-Z XL board as seen in Fig. 5. The use of wet electrodes was to reduce additional sources of noise while maintaining a focus on sensing electrode configurations rather than injection electrode configurations. Like ΔBio-Z, PTT measurements were normalized between 0 – 1. We used the measured PTT amplitudes to comment on the specificity of bioimpedance sensing for different electrode configurations.

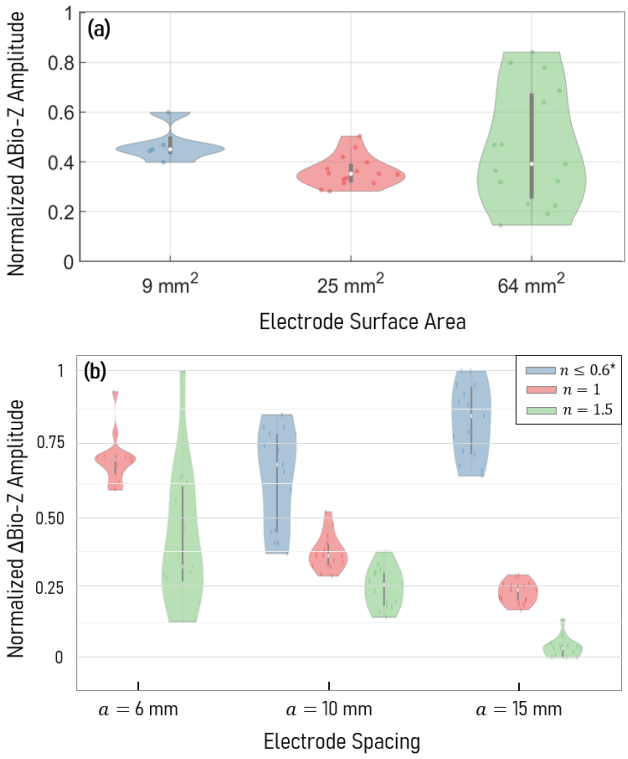

Figure 6. (a) Change in ΔBio-Z amplitude with changing electrode contact area. The white dot and black bar indicate the mean and 25th to 75th percentile data range, respectively. The width of the plot demonstrates the distribution of data points at the corresponding normalized amplitude. (b) Change in ΔBio-Z amplitude with electrode spacing for Wenner (i.e., $n = 1$) and Wenner-Schlumberger configurations. *n = 0.6 for a = 10 mm and n = 0.5 for a = 15 mm.

III. Results and Discussion

We recruited three young, healthy participants under the IRB approval IRB2017-0086D by Texas A&M University. We obtained five repetitions of one-minute ΔBio-Z and PTT measurements for each participant, with participants at rest.

A. Electrode-skin impedance with varying frequency and contact area

The electrode-skin impedance values for each frequency amongst subjects were averaged together and shown in Fig. 3. We observe a decrease in the contact impedance with increasing frequency and increasing contact area. These results are consistent with previous reports [14], as the electrode-skin interface for dry electrodes exhibits a large capacitive component due to air gaps at the skin surface and a large resistive component due to the low conductivity of the stratum corneum, often modeled as a resistor and capacitor in parallel [15]. At the operating frequency used in this study for ΔBio-Z and PTT measurements (*i.e.*, 13.4 kHz) we measured the contact impedance as 16.8 kΩ, 7.1 kΩ, and 4.1 kΩ for 9 mm², 25 mm², and 64 mm² contact areas, respectively. This shows that there is a much greater risk of excitation signal saturation for 9 mm² electrodes than for 25 mm² and 64 mm² electrodes.

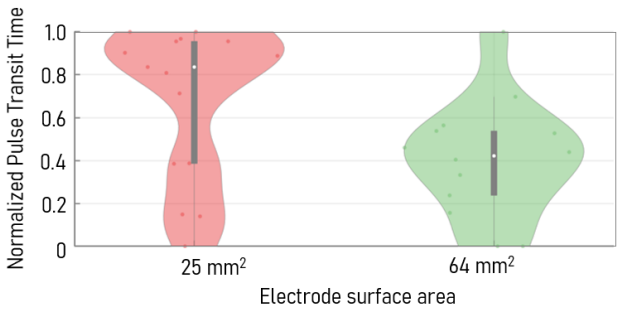

Figure 7. Change in pulse transit time magnitude with changing electrode contact area. Note the normalized amplitude, as each participant exhibited different pulse transit times.

B. Biompedance sensitivity measurements with varying electrode spacing and area

An increase in measured ΔBio-Z directly increases the signal-to-noise ratio of the system and can be attributed to an increase in sensitivity around the artery. Thus, it is beneficial to increase the localization around the artery and provide the cleanest signal.

An increase in electrode contact area among arrays with equal on-center spacings caused a drop in measured ΔBio-Z, as seen in Fig. 6a. This observation agrees with previous reports [8] and may be due to a decrease in the amplitude of the current traveling into the artery, due to some of the injected current leaking to the neighboring tissues. It should be noted, however, that one subject experienced substantially higher amplitude for 64mm² electrodes, which leads us to believe that wrist anatomy among subjects plays a role in conjunction with the sensitivity fields produced by the range of electrode sizes used in the study.

We observed an apparent drop in the ΔBio-Z amplitude with an increasing spacing coefficient for Wenner-Schlumberger configurations, as shown in Fig. 6b. Like the decrease in ΔBio-Z amplitude seen for increasing sizes, this is speculatively due to the leakage of the electric current to the neighboring tissues and cells, as well as the secondary artery (*i.e.,* ulnar artery) leading to a less localized measurement of the pulse traveling across the radial artery. Therefore, results suggest that a decrease in the spacing between excitation electrodes yields a higher sensitivity to the underlying pulsatile activity, in addition to its advantageous reduced form-factor. However, increasing the spacing between voltage sensing electrodes when excitation electrodes maintained close spacings to sensing electrodes (i.e., 1 – 2.5 mm) produced higher ΔBio-Z amplitudes. Thus, to obtain the best signal, a wearable bioimpedance system may benefit from minimizing excitation electrode spacings while increasing sensing electrode spacings within form-factor constraints. Another interesting trend observed is the increase from a = 10 mm to a = 15 mm for n = 0.5/0.6, while other values of n show a decrease in ΔBio-Z amplitude with an increase in a. This is an indication that, in this range, a higher ratio between sensing and injection electrode spacings

may tend to yield higher ΔBio-Z amplitudes as the sensing electrode spacing increases.

Our findings suggest that the measured ΔBio-Z for small-sized, silver dry electrodes aligned with the radial artery generally benefit from compact spacing between current injecting and voltage sensing electrodes and decreased surface area. This decreased surface area, however, leads to noticeably larger skin-electrode impedances. The increased skin impedances could lead to saturation of the excitation signal or too large of a voltage drop over the skin layer, leading to a minimal voltage difference across the artery. Thus, while decreasing electrode surface area may be beneficial for localization effects, it presents limitations on hardware components for both excitation signal injection and sampling.

C. Pulse-Transit Time (PTT) assessment

We conducted PTT experiments for two different electrode configurations (surface areas: 25 mm^2, 64 mm^2), both yielding a total sensor width of 30 mm measured across on-center spacings. The result to this analysis is shared in Fig. 7. We observed that the increase in electrode contact area from 25 mm^2 to 64 mm^2 decreases the mean PTT from a normalized value of 0.67 to 0.41. This could indicate that PTT measurements, and therefore the specificity of bioimpedance sensing, may benefit from a decreased electrode surface area.

IV. Conclusion

In this study, we presented a thorough experimental analysis of the bioimpedance modality with varying sizes and spacings for dry electrodes used to establish skin contact. Our findings indicate that smaller sensor sizes can still obtain a high-quality bioimpedance signal and show reproducible trends. We found that trends associated with smaller electrode sizes (*e.g.*, 9 mm^2), decreased excitation electrode spacings, and increased voltage sensing electrode spacings indicate a better signal-to-noise ratio when measuring ΔBio-Z, with a trade-off of higher skin-contact impedance when using smaller electrodes. Future research would benefit from a deeper look into frequency and size analysis to produce a minimal form factor with high spatial resolution, as well as a morphological assessment of Bio-Z signals with varying electrode configurations. Furthermore, this work may benefit from a future study incorporating more participants, allowing for a statistical rather than trend-centered analysis while also considering factors such as BMI, skin hydration levels, and other such metrics that may affect results.

Acknowledgment

This work was supported in part by the National Institutes of Health, under grant 1R01HL151240-01A1. Any opinions, findings, conclusions, or recommendations expressed in this material are those of the authors and do not necessarily reflect the views of the funding organizations.

References

[1] K. Vijayalakshmi, S. Uma, R. Bhuvanya, and A. Suresh, "A demand for wearable devices in health care," *Int. J. Eng. Technol.*, vol. 7, no. 1.7, pp. 1–4, 2018.

[2] J. Allen, "Photoplethysmography and its application in clinical physiological measurement," *Physiol. Meas.*, vol. 28, no. 3, p. R1, 2007.

[3] B. Ibrahim and R. Jafari, "Cuffless blood pressure monitoring from an array of wrist bio-impedance sensors using subject-specific regression models: Proof of concept," *IEEE Trans. Biomed. Circuits Syst.*, vol. 13, no. 6, pp. 1723–1735, 2019.

[4] K. Sel, A. Brown, H. Jang, H. M. Krumholz, N. Lu, and R. Jafari, "A Wrist-worn Respiration Monitoring Device using Bio-Impedance," in *2020 42nd Annual International Conference of the IEEE Engineering in Medicine \& Biology Society (EMBC)*, 2020, pp. 3989–3993.

[5] R. Ben Salah, T. Alhadidi, I. Ben Salah, and K. Ouni, "Non-invasive determination of the arterial compliance by cardiovascular bioimpedance signal processing," in *2018 IEEE 20th International Conference on e-Health Networking, Applications and Services (Healthcom)*, 2018, pp. 1–6.

[6] M. Park, K. Eom, M. H. Jung, Y. S. Park, J.-Y. Lee, and S. H. Nam, "Design of Bio-Impedance Electrode Topologies for Specific Depth Sensing in Skin Layer," in *2020 42nd Annual International Conference of the IEEE Engineering in Medicine \& Biology Society (EMBC)*, 2020, pp. 3961–3964.

[7] K. Pesti, M. Metshein, P. Annus, H. Kõiv, and M. Min, "Electrode placement strategies for the measurement of radial artery bioimpedance: Simulations and experiments," *IEEE Trans. Instrum. Meas.*, vol. 70, pp. 1–10, 2020.

[8] T.-W. Wang *et al.*, "Bio-impedance measurement optimization for high-resolution carotid pulse sensing," *Sensors*, vol. 21, no. 5, p. 1600, 2021.

[9] M. G. Srinivasa and P. S. Pandian, "Dry electrodes for bio-potential measurement in wearable systems," in *2017 2nd IEEE International Conference on Recent Trends in Electronics, Information \& Communication Technology (RTEICT)*, 2017, pp. 270–276.

[10] S. Grimnes and Ø. G. Martinsen, "Bioimpedance," *Wiley Encycl. Biomed. Eng.*, 2006.

[11] R. Kusche, S. Kaufmann, and M. Ryschka, "Dry electrodes for bioimpedance measurements—design, characterization and comparison," *Biomed. Phys. \& Eng. Express*, vol. 5, no. 1, p. 15001, 2018.

[12] Medical electrical equipment Part 1: General requirements for basic safety and essential performance ANSI/AAMI ES60601- 1:2005/A1:2012.

[13] B. Ibrahim, A. Akbari, and R. Jafari, "A novel method for pulse transit time estimation using wrist bio-impedance sensing based on a regression model," in *2017 IEEE Biomedical Circuits and Systems Conference (BioCAS)*, 2017, pp. 1–4.

[14] K. Sel, D. Kireev, A. Brown, B. Ibrahim, D. Akinwande, and R. Jafari, "Electrical characterization of graphene-based e-tattoos for bio-impedance-based physiological sensing," in *2019 IEEE Biomedical Circuits and Systems Conference (BioCAS)*, 2019, pp. 1–4.

[15] K. Sel, J. Zhao, B. Ibrahim, and R. Jafari, "Measurement of chest physiological signals using wirelessly coupled bio-impedance patches," in *2019 41st Annual International Conference of the IEEE Engineering in Medicine and Biology Society (EMBC)*, 2019, pp. 376–381.